


Feshbach resonances of large-mass-imbalance Er-Li mixturesF. Schäfer^{✉,*}, N. Mizukami,[†] and Y. Takahashi[✉]*Department of Physics, Graduate School of Science, Kyoto University, Kyoto 606-8502, Japan* (Received 14 November 2021; accepted 17 December 2021; published 24 January 2022)

We report on the experimental observation of Feshbach resonances in large-mass-imbalance mixtures of erbium (Er) and lithium (Li). All combinations of ^{168}Er , ^{166}Er , and ^7Li , ^6Li are cooled to temperatures of a few microkelvin, partially by means of sympathetic cooling together with ytterbium (Yb) as a third mixture component. The Er-Li inelastic interspecies collisional properties are studied for magnetic fields up to 680 G. In all cases, resonant interspecies loss features, indicative of Feshbach resonances, have been observed. While most resonances have sub-Gauss widths, a few of them are broad and feature widths of several Gauss. Those broad resonances are a key to the realization of ultracold Er-Li quantum gas mixtures with tunable interactions.

DOI: [10.1103/PhysRevA.105.012816](https://doi.org/10.1103/PhysRevA.105.012816)**I. INTRODUCTION**

Ultracold quantum gases are by now an established and indispensable means to manipulate, probe, and study the intricate behavior of quantum matter as, for example, impressively demonstrated in the realization of strongly correlated quantum many-body systems [1] as well as few-body systems [2]. In many cases, experiments are facilitated by use of Feshbach resonances that give rise to the necessary fine-tuned control of atomic interactions [3]. Landmark experiments demonstrating the crossover from Bardeen-Cooper-Schrieffer (BCS) pairing to a Bose-Einstein condensate (BEC) [4] and Efimov trimer-state series [5] are due to that minute interaction control mechanism. Finally, going from single-component to dual-species experiments, the realm of accessible physics is further broadened and allows as a direct application the simulation of impurity problems [6,7] and the study of polaron physics [8] but also more intricate applications such as the production of ultracold heteronuclear molecules [3], mixed-species Efimov trimer physics with reduced scaling constants [2], and chiral p -wave superfluids [9,10]. It is important to note that in the preceding last two examples the effects, while rendered possible already by the presence of two different species, can be crucially enhanced by use of large-mass-imbalance mixtures. There, a large mass ratio is the driving force in the reduction of Efimov scaling constants and a deciding factor in bringing the superfluid critical temperature into experimentally accessible realms.

We here present our first results of the experimental realization of a large-mass-imbalance mixture of heavy erbium (Er) and light lithium (Li) atoms and the discovery of interspecies Feshbach resonances. In previous experiments, much effort was spent on similar investigations in ultracold mixtures of heavy ytterbium (Yb) and light Li [11–13]. While these works

scanned a large range of isotope combinations, electronic configurations, and magnetic field strengths, only a few traces of Feshbach resonances could be detected with limited applicability toward an efficient control of interspecies interactions. In that respect, Er seems a formidable candidate to remedy these shortcomings of Yb-Li mixtures. While generally being comparable in mass to the heavy lanthanide Yb, it has the distinct properties of a very large magnetic moment giving rise to strong dipole-dipole interactions and the existence of nonzero orbital angular momentum states. As such, successful efforts to create quantum degenerate gases of Er have already occurred 10 years ago [14] and led to the unveiling of dense Er-Er Feshbach spectra akin to chaotic behavior [15]. Further theoretical work revealed the strong possibility of a rich Feshbach physics in Er-Li mixtures [16], which is the subject of the present experimental work. Starting with the bosonic isotopes of either ^{168}Er or ^{166}Er and either bosonic ^7Li or fermionic ^6Li , we are now able to identify a variety of resonantly enhanced inelastic scattering losses between Er and Li at microkelvin temperatures. The purpose of the present work is, after summarizing the experimental method in Sec. II and apart from generally reporting on the observation of Er-Li interspecies Feshbach resonances, to give a succinct overview of the accessible parameters and the range of observable resonances (Sec. III). We conclude in Sec. IV by discussing the range of possible applications of such a large-mass-imbalance mixture with tunable interspecies interactions.

II. EXPERIMENT

The experiment is based on our Yb-Li machine described previously [17,18]. In an upgrade of the experiment, a high-temperature oven for Er has additionally been added to the setup, giving us the freedom to work with either single species or with arbitrary combinations of Er, Yb, and Li in dual- or triple-species mixtures. The Er part of the setup and experimental sequence largely follows the established techniques [14]. From the Er source heated to about 1050 °C, a hot atomic beam is formed. A transversal cooling stage operating

*schaefer@scphys.kyoto-u.ac.jp

[†]Present address: European Laboratory for Nonlinear Spectroscopy (LENs), Via Nello Carrara 1, 50019 Sesto F. no (FI), Italy.

on the broad $4f^{12}6s^2(^3H_6)$ to $4f^{12}(^3H_6)6s6p(^1P_1)$ transition at 401 nm limits the initial transverse spread to the thermal Er beam. A subsequent Zeeman slowing stage operating on the same transition reduces the longitudinal velocity of the Er atoms. A magneto-optical trap (MOT) operating on the narrow $4f^{12}6s^2(^3H_6)$ to $4f^{12}(^3H_6)6s6p(^3P_1)$ intercombination line at 583 nm forms the initial trapping stage. From there, the atoms are transferred into a far-off-resonant optical trap (FORT) of crossed, focused beams at 1064 and 1070 nm. It is known that due to the narrow linewidth of the transition at 583 nm of 186 kHz and the resulting displacement of the heavy Er atoms from the center of the MOT by gravitational pull the atomic state is automatically polarized in the lowest angular momentum sublevel [14], $m_j = -6$ in the case at hand. By maintaining a sufficiently strong magnetic field for a well-defined quantization axis during the following forced evaporation period, this polarized state is maintained throughout the experiment. Evaporation typically starts at 1.2 G to prevent depolarization by thermal excitation and the field is lowered to 0.4 G once the sample is sufficiently cold for more favorable collisional properties and better evaporation efficiency. Following the technique outlined in Ref. [19], the polarization state has been confirmed via absorption imaging on the narrow 583-nm line, which at moderate magnetic bias fields of about 20 G and low imaging light intensities is selective to a single spin state only. Trapping and cooling of either ^7Li or ^6Li is performed as previously reported [17,20] including optical pumping of Li during the initial stage of the evaporation process to a spin-stretched ground state. Successful spin polarization is confirmed by the Stern-Gerlach technique, that is, standard absorption imaging after short application of a magnetic field gradient to spatially separate the m_F hyperfine magnetic sublevels. The accessible stretched states are $F = 1/2$, $m_F = \pm 1/2$ for ^6Li and $F = 1$, $m_F = \pm 1$ for ^7Li . Additionally, when investigating ^{168}Er - ^7Li , a third loading stage of ^{174}Yb has been added to the experiment. Due to the very efficient evaporation of ^{174}Yb and by virtue of sympathetic cooling of both ^{168}Er and ^7Li , larger and colder mixtures can be achieved. The remaining Yb atoms are then removed before the actual Feshbach resonance measurement by a short pulse of light resonant to the 1S_0 - 1P_1 transition of ^{174}Yb .

Forced evaporation of the two- or three-species mixture is done by suitably lowering the intensities of the FORT lasers within 8 s (10 s when sympathetically cooled by Yb). After that time, we typically obtain an Er-Li mixture with 2×10^4 to 5×10^4 Er atoms and 5×10^3 to 15×10^3 Li atoms. The actual atom number depends on the chosen isotope combination, the desired final temperatures, and the day-to-day performance details of the experiment. The sample is non-degenerate and in the absence of sympathetic cooling with Yb its temperature is found between 2 and 5 μK , with Er typically being about 1 μK colder than Li. This demonstrates both that Er sympathetically cools down Li and that during the last stages of the evaporation the transfer of thermal energy between the species becomes less efficient, which is similar to former experience in Yb-Li mixtures [21], whereas in Yb-assisted sympathetic cooling of ^{168}Er - ^7Li temperatures as low as 0.5 μK are observed. The expected trap frequencies are about $(\omega_x, \omega_y, \omega_z) = 2\pi \times (420, 100, 50)$ Hz for Er and

$2\pi \times (2640, 610, 300)$ Hz for Li, with the z axis being in the vertical direction. In that condition, the difference in the trap centers due to gravitational sag is about 1.4 μm , which is sufficiently less than typical atom cloud dimensions in vertical direction of about 6 μm and is thus negligible for the purposes of the present work.

The main part of the experimental sequence is to detect magnetic-field-dependent changes in the interspecies inelastic collision rates in a trap-loss sequence. For this, after the initial preparation of the desired cold mixture sample, a homogeneous magnetic field is linearly ramped up to the target value within 10 ms, sufficiently slow to allow the magnetic field control system to adjust the magnetic field without significant under- or overshoots. The system is then kept in this condition for 500 ms. During this time, inelastic collisions between the atoms lead to a reduction of the number of atoms in the optical trap. The magnetic field value is stabilized via a feedback signal from a current sensor on the magnetic coil that acts on an insulated-gate bipolar transistor (IGBT). The absolute magnetic field value is found by characterizing the narrow s -wave Feshbach resonance [22] of ^6Li at 543.28(8) G and we assume linearity of the setup for other field values. Comparing our data for ^{168}Er - ^{168}Er Feshbach resonances at low magnetic fields to those presented in Ref. [15], we find agreement in the observed resonance positions to within 0.3 G. This systematic uncertainty is the major contribution to our measurement error and outweighs the high frequency noise of our magnetic field, which is estimated to be about 0.02 G, and any magnetic field inhomogeneities, which are expected to be of similar order. The magnetic field resolution is limited by the setpoint resolution of the employed 16-bit digital-to-analog control front-end to about 0.03 G. After the holding time at the target magnetic field, the current in the magnetic coils is ramped down to zero in 10 ms and the system is kept there for another 10 ms to allow for eventual residual fields due to eddy currents to decay. In standard time-of-flight absorption imaging, we then image the remaining Er atoms after 2 ms and the Li atoms after 0.3 ms of free expansion. Additionally, for every magnetic field setting of this main sequence, we interleave additional control measurements in which either of the two species is removed from the optical trap by a short pulse of resonant 583 nm (Er) or 671 nm (Li) light before starting the magnetic field sequence. These measurements serve as reference points to distinguish losses due to interspecies collisions from those caused by single-species-only interactions. Finally, while these data are obtained every 60 or 180 mG, typically every 1 G additional data of the mixture is taken where the magnetic field is kept constantly low. This is to better detect possible drifts of the overall atom numbers or general changes in the performance of the experimental setup.

III. RESULTS

In the following, we give an overview of the data obtained in the experiment. This is to demonstrate the range of typically observed resonance shapes and their densities and dependence on isotope and spin combinations.

We first take a look at the general isotope and hyperfine spin-state dependence of the Feshbach spectra. Figure 1 shows

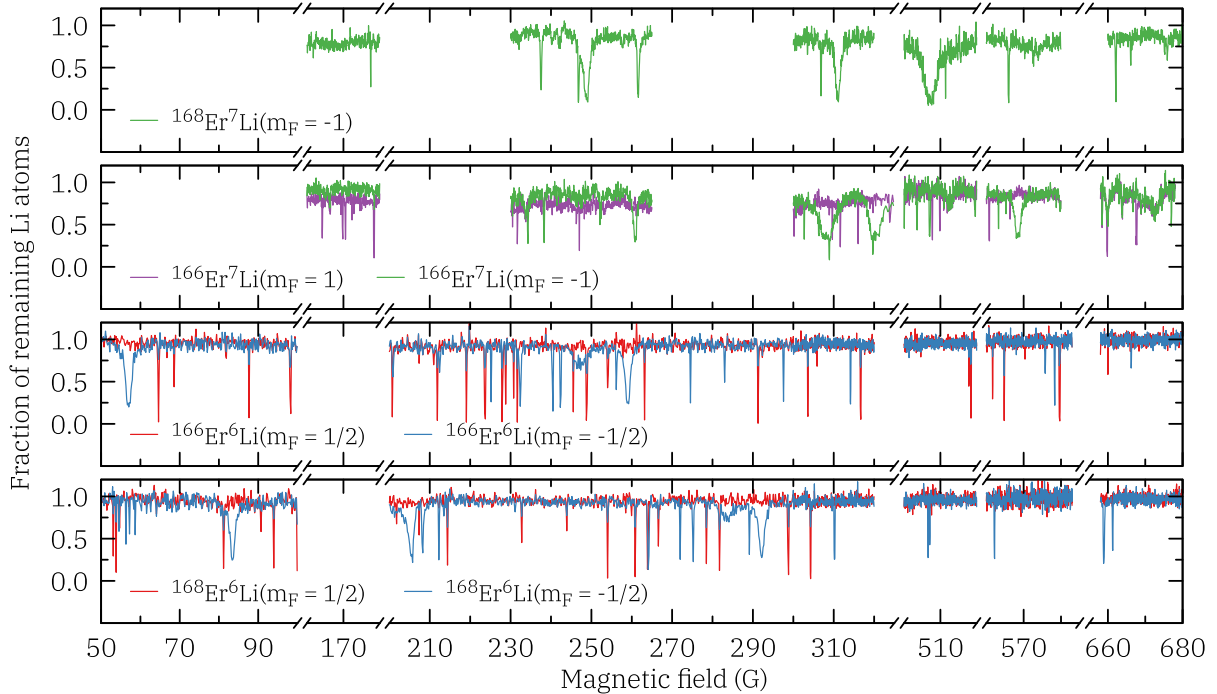


FIG. 1. Magnetic field dependence of Li atom losses for various Er-Li mixtures. The four different panels show the fraction of remaining Li atoms for four Er-Li isotope combinations after 500 ms interaction time at magnetic fields between 50 and 680 G. (Note that the magnetic field axis is not continuous as some magnetic field ranges without data are omitted.) In each case, Li has been optically pumped to one of the two stretched state configurations (see panel labels) and Er is always spin polarized into the $m_J = -6$ ground state. Each data point is the averaged ratio of typically three measurements with and without Er. Many narrow and some broad resonant loss features are observed.

for the magnetic field range 50 to 680 G trap-loss spectra of all isotope and spin combinations that could be investigated in the present work. The spectra are taken at a magnetic field resolution between 60 and 180 mG. In each case, we report the fractional loss of Li atoms expressed as the ratio of atoms remaining in the trap after the interaction time for the Er-Li mixture case compared to the case of Li atoms only in the trap. While it was not possible to maintain constant absolute atom numbers across all experiments, between measurements of different isotope combinations or magnetic field ranges the overall atom numbers are typically reproduced to within about 30%. Note that for brevity we will in the following suppress $m_J = -6$ in the quantum state description of Er and $F = 1/2$ ($F = 1$) for ${}^6\text{Li}$ (${}^7\text{Li}$); they are to be understood implicitly. We further need to point out that for ${}^{168}\text{Er}$ ${}^7\text{Li}$ (top panel) we were not able to create a cold mixture of ${}^{168}\text{Er}$ ${}^7\text{Li}(m_F = 1)$. Even though at the beginning of the evaporation ramp such a mixture could be produced, the ${}^7\text{Li}(m_F = 1)$ atoms are rapidly lost during the evaporation sequence. Also, no magnetic bias field could be found that allows for both efficient evaporation and collisional stability of the mixture, indicating the existence of a broad resonance at only a few Gauss for this isotope and hyperfine spin-state combination. This is especially interesting as the energetically lowest state in ${}^7\text{Li}$ is the $m_F = 1$ state and naively one would expect this state to be most stable toward possible inelastic processes. Instead, it is the energetically higher $m_F = -1$ state that can be prepared in the experiment. The data in the top panel of Fig. 1 therefore only show the ${}^{168}\text{Er}$ ${}^7\text{Li}(m_F = -1)$ mixture. The other isotope combinations (remaining panels) do not suffer from

such a limitation. The available data do not cover the complete magnetic field range (note the omission marks in the magnetic field scale in Fig. 1) and only a total range of between roughly 150 G (${}^7\text{Li}$) and 250 G (${}^6\text{Li}$) was scanned for each mixture. The selection of the possibly interesting magnetic field regions has been guided by the predictions of Ref. [16]. As such, with a continuous measurement time of about a week per isotope and hyperfine spin combination, a good overview of the spectral properties has been obtained. Each mixture features a distinct resonance structure of numerous narrow and several broader resonances. A detailed list of all observed resonance positions and their widths is provided in Table I. While the broader Feshbach resonances can be induced by ordinary s -wave coupling, the numerous observed narrow resonances may be understood as a result of anisotropy-induced Feshbach resonances where the anisotropy originates from the electrostatic interaction between Er and Li [16,23]. It seems further worth mentioning that there is an apparent lack of broad Feshbach resonances with Li in the energetically lowest magnetic sublevel [${}^7\text{Li}(m_F = +1)$ and ${}^6\text{Li}(m_F = +1/2)$], which is not reflected in current calculations [16]. Further experimental efforts will be necessary, however, to further corroborate such observations.

We now turn to a discussion of the structures of individual resonances. The panels of Fig. 2 display in the mixture of ${}^{168}\text{Er}$ ${}^7\text{Li}(m_F = -1)$ a narrow Feshbach resonance at low magnetic fields around 15.8 G and a particularly broad resonance at higher fields around 510 G. In both cases, the mixture sample is prepared at a temperature of about $2.0 \mu\text{K}$ for ${}^{168}\text{Er}$ and $2.7 \mu\text{K}$ for ${}^7\text{Li}$. In the vicinity of 15.8 G, Fig. 2(a)

TABLE I. List of identified Er-Li interspecies Feshbach resonances. The resonance positions B_0 and their widths ΔB are given as determined by fits of squared Breit-Wigner lineshapes to the Li loss data shown in Fig. 1. Within the present experiments, no reliable width determination is possible for very narrow resonances and those resonances with widths below 100 mG are here indicated by <100 . Further, only resonances that are either reasonably broad or that cause a loss of Li atoms by at least one third are listed. Where imperfect optical pumping causes seemingly simultaneous losses in both Li spin states, the resonance is attributed to the dominant spin component only. Resonances that are marginal for the identification are also included but put in brackets. Note that for $B > 50$ G only resonances within the investigated magnetic field ranges (cf. Fig. 1) are listed and that due to the finite magnetic field step size some very narrow resonances might not have been detected. Below 50 G, some additional resonances are included that have been found in separate measurements.

Mixture	B_0 (G)	ΔB (mG)
$^{168}\text{Er } ^7\text{Li}(m_F = -1)$	1.7	<100
	7.5	<100
	15.8	100
	177.5	<100
	237.6	300
	246.8	300
	248.8	1600
	261.6	500
	306.8	200
	311.1	1400
	507.3	4000
	511.4	<100
	566.0	200
	662.1	200
	666.1	200
	675.9	300
$^{166}\text{Er } ^7\text{Li}(m_F = 1)$	13.1	400
	16.8	<100
	164.2	100
	169.8	100
	170.6	100
	178.4	200
	231.7	<100
	233.6	700
	247.0	<100
	300.2	100
	309.6	<100
	311.6	<100
	316.0	100
	507.8	100
	509.9	<100
	(512.4)	(2300)
	560.8	100
	566.4	<100
	658.5	<100
	659.8	300
663.7	300	
667.6	300	
(672.4)	(3200)	
$^{166}\text{Er } ^7\text{Li}(m_F = -1)$	23.6	130
	233.8	500
	234.3	200

TABLE I. (Continued.)

Mixture	B_0 (G)	ΔB (mG)
	238.3	200
	260.8	900
	300.7	<100
	302.7	<100
	306.3	<100
	308.5	4900
	308.9	100
	319.8	100
	319.9	3200
	500.1	<100
	503.6	300
	507.1	300
	(512.4)	(1700)
	519.5	400
	563.3	<100
	565.3	<100
	568.4	1800
	658.4	100
	663.7	500
	(672.4)	(4000)
677.0	<100	
$^{166}\text{Er } ^6\text{Li}(m_F = 1/2)$	18.9	<100
	22.1	<100
	25.6	<100
	26.3	<100
	37.8	<100
	64.6	200
	68.6	<100
	87.7	<100
	98.2	<100
	200.8	<100
	211.9	100
	219.1	100
	223.7	<100
	228.0	<100
	228.8	100
	230.8	<100
231.7	100	
245.5	<100	
248.9	<100	
254.1	<100	
263.2	<100	
291.3	<100	
303.6	<100	
(305.9)	(<100)	
316.7	200	
517.9	<100	
518.4	100	
561.7	<100	
564.8	100	
(570.4)	(100)	
579.6	200	
660.0	<100	
$^{166}\text{Er } ^6\text{Li}(m_F = -1/2)$	13.3	<100
	20.9	<100
	24.0	<100
	26.7	100
	32.7	<100

TABLE I. (Continued.)

Mixture	B_0 (G)	ΔB (mG)
	57.0	1700
	212.5	300
	225.2	<100
	232.4	400
	240.4	<100
	242.4	<100
	247.0	4200
	256.2	<100
	259.0	1300
	274.5	<100
	283.0	200
	297.5	<100
	314.1	<100
	575.8	200
	578.3	100
	666.2	<100
$^{168}\text{Er}^6\text{Li}(m_F = 1/2)$	23.2	<100
	(42.5)	(<100)
	46.4	100
	53.1	<100
	53.8	<100
	54.7	<100
	81.2	200
	90.7	<100
	93.9	200
	201.8	<100
	207.4	<100
	214.4	<100
	232.8	100
	243.9	100
	254.0	<100
	260.9	<100
	264.0	<100
266.6	100	
278.5	<100	
281.8	<100	
298.7	<100	
304.3	200	
$^{168}\text{Er}^6\text{Li}(m_F = -1/2)$	31.2	100
	35.4	<100
	41.5	<100
	(42.5)	(<100)
	54.6	<100
	56.3	<100
	57.2	<100
	58.7	<100
	83.4	1500
	205.5	1800
	208.1	300
	212.3	<100
	264.2	<100
	272.0	<100
	275.2	200
	283.1	4300
	289.1	<100
292.2	1500	
310.2	200	
506.6	<100	

TABLE I. (Continued.)

Mixture	B_0 (G)	ΔB (mG)
	507.1	100
	562.2	100
	658.9	300
	661.3	100

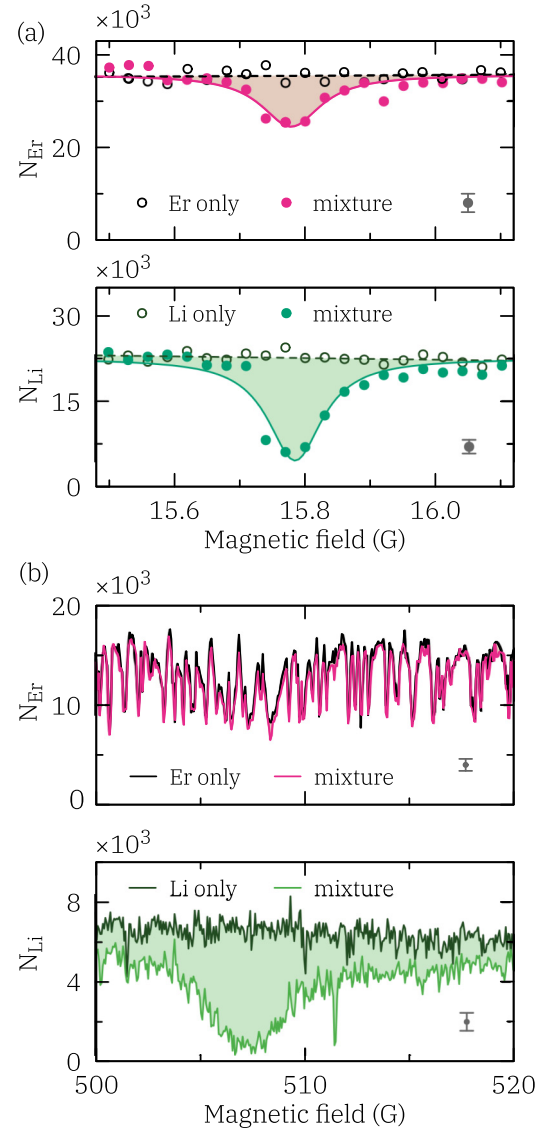


FIG. 2. Detailed view of two $^{168}\text{Er}^7\text{Li}(m_F = -1)$ interspecies Feshbach resonances. The data acquisition and organization of each panel are as in Fig. 1. The typical statistical error of the displayed mean data is indicated in each panel by a single error bar example (dark gray). (a) At about 15.8 G, a narrow Feshbach resonance is observed. Resonant losses of Er and Li atoms are observed only in the mixture case; single-species data show no loss indications. The solid (dashed) line indicates a Breit-Wigner (straight line) fit to the data and gives a FWHM width of about 0.1 G. The interaction time at each magnetic field was, different from the remaining experiments, set to only 10 ms. (b) At about 507 G, a broad interspecies Feshbach resonance with a width of about 4 G is found and the resonant losses in ^7Li are dominantly visible. The additional losses in the complicated structure of ^{168}Er are only barely observable. At 511 G, an additional, very narrow interspecies loss feature is resolved.

shows a narrow interspecies Feshbach resonance with a full width at half maximum (FWHM) of about 0.1 G. In the shown magnetic field range, the single-species data (open symbols), where the atoms of the other species were removed from the trap before setting the magnetic field, is featureless. In the mixture, however, a coinciding loss of both Er and Li is visible, indicative of the enhanced inelastic losses of an interspecies Feshbach resonance. As the interaction time for that particular experiment has been set to only 10 ms, the inelastic losses seem unusually large for this particular resonance. Note that the remaining experiments reported in the present work operate at a holding time of 500 ms. In the higher magnetic field range of Fig. 2(b), looking first at the ^{168}Er data, the dominant and previously reported dense structure of Er-Er Feshbach resonances is evident [15]. Going to the ^7Li data again, the resonance structure relevant to the present research is revealed: While the “Li only” data shows only a smooth variation in the overall atom number that can be fully attributed to a drift of the general performance of the experiment, the data of the mixture clearly display a broad resonant loss. In contrast to the data at 15.8 G, the interspecies loss is this time only weakly reflected in the Er data. This is partially due to a reduced visibility caused by the dense Er-Er Feshbach resonance structure but is expected to also be induced by the large mass imbalance between the two species. Differences between predominantly two-body collisional losses and three-body collisional resonances might further contribute to the qualitative change in the observed Er losses. The resonance shape is asymmetric and we extract an approximate resonance position and FWHM by a Lorentzian fit to the ^7Li data. We find a resonance position of 507.3 G and a FWHM of 4.0 G. This broad resonance is accompanied by a very narrow one at 511.4 G that has a width well below 0.1 G at the limit of our experimental resolution.

IV. DISCUSSION AND CONCLUSION

With the present set of experimental results, we demonstrate the realization of large-mass-imbalance mixtures of Er and Li in various isotopic combinations. While not seamlessly exploring the complete magnetic field range up to 680 G, we focus on a more detailed investigation of the Er-Li interspecies Feshbach resonance structure in multiple field locations. Making best use of our limited machine time, this approach is chosen to obtain a general idea of the expected spectra and to better support theoretical efforts in the modeling and understanding of the Feshbach spectra by providing data samples

over a possibly large range of magnetic fields and isotope and spin combinations. As expected, we find a wealth of interspecies Feshbach resonances at a density of about one resonance per ten Gauss, most of them quite narrow, some of them with widths beyond 1 G. This encouraging overall consistency between the observed Feshbach resonance spectra and current theory predictions [16] is contrasted by the lack of a detailed understanding of both the exact resonance structures and the character of their collisional interactions. Joint efforts of both experiment and theory will be necessary for a better grasp of this complicated system. Additionally, the present work reveals mixture lifetimes on the order of up to 1 s even at resonance. This is, e.g., about two orders of magnitude longer than inelastic collision rate limited lifetimes found in the large mass-imbalance system of $\text{Yb}(^3\text{P}_2)\text{-Li}$ [12] and an encouraging starting point for further research of Er-Li mixtures in the strongly interacting regime.

To our knowledge, this mixture system currently represents the largest experimentally realized mass-imbalanced mixture with tunable interactions. Additional measurements are in preparation to precisely determine the binding energies of the corresponding Feshbach molecules. Considering in particular a similar kind of mixture of heavy ^{167}Er fermions and light ^7Li bosons, this opens the road to three-body Efimov states with both reduced scaling constants and nonvanishing angular momenta [2] and chiral p -wave superfluids in mixed dimensions. Additionally, ultracold mixtures of Yb and Er should allow for a detailed study of mass-scaling effects in Yb-Er Feshbach resonances [24]. Ultracold triple-species quantum gas mixtures of ytterbium, erbium, and lithium are also within reach.

ACKNOWLEDGMENTS

We thank Y. Takasu for early experimental assistance and useful discussions, K. Aikawa for helpful advice in early stages of the experiment, and P. Żuchowski for fruitful discussions of the Feshbach spectra and for sharing his theoretical insight with us. N.M. acknowledges support from the JSPS (KAKENHI Grant No. 21J20153). This work was supported by the Grants-in-Aid for Scientific Research of JSPS Grants No. JP17H06138, No. 18H05405, and No. 18H05228; JST CREST Grant No. JPMJCR1673 and the Impulsing Paradigm Change through Disruptive Technologies (ImPACT) program by the Cabinet Office, Government of Japan; and MEXT Quantum Leap Flagship Program (MEXT Q-LEAP) Grant No. JPMXS0118069021.

-
- [1] I. Bloch, J. Dalibard, and W. Zwerger, *Rev. Mod. Phys.* **80**, 885 (2008).
 - [2] P. Naidon and S. Endo, *Rep. Prog. Phys.* **80**, 056001 (2017).
 - [3] C. Chin, R. Grimm, P. Julienne, and E. Tiesinga, *Rev. Mod. Phys.* **82**, 1225 (2010).
 - [4] M. Randeria and E. Taylor, *Annu. Rev. Condens. Matter Phys.* **5**, 209 (2014).
 - [5] M. Zaccanti, B. Deissler, C. D’Errico, M. Fattori, M. Jonas, S. Müller, G. Roati, M. Inguscio, and G. Modugno, *Nat. Phys.* **5**, 586 (2009).
 - [6] P. W. Anderson, *Phys. Rev.* **109**, 1492 (1958).
 - [7] J. Kondo, *Prog. Theor. Phys.* **32**, 37 (1964).
 - [8] C. Kohstall, M. Zaccanti, M. Jag, A. Trenkwalder, P. Massignan, G. M. Bruun, F. Schreck, and R. Grimm, *Nature (London)* **485**, 615 (2012).
 - [9] Y. Nishida, *Ann. Phys.* **324**, 897 (2009).
 - [10] Y.-J. Wu, J. He, C.-L. Zang, and S.-P. Kou, *Phys. Rev. B* **86**, 085128 (2012).
 - [11] W. Dowd, R. J. Roy, R. K. Shrestha, A. Petrov, C. Makrides, S. Kotochigova, and S. Gupta, *New J. Phys.* **17**, 055007 (2015).

- [12] F. Schäfer, H. Konishi, A. Bouscal, T. Yagami, and Y. Takahashi, *Phys. Rev. A* **96**, 032711 (2017).
- [13] A. Green, H. Li, J. H. See Toh, X. Tang, K. C. McCormick, M. Li, E. Tiesinga, S. Kotochigova, and S. Gupta, *Phys. Rev. X* **10**, 031037 (2020).
- [14] K. Aikawa, A. Frisch, M. Mark, S. Baier, A. Rietzler, R. Grimm, and F. Ferlaino, *Phys. Rev. Lett.* **108**, 210401 (2012).
- [15] A. Frisch, M. Mark, K. Aikawa, F. Ferlaino, J. L. Bohn, C. Makrides, A. Petrov, and S. Kotochigova, *Nature (London)* **507**, 475 (2014).
- [16] M. L. González-Martínez and P. S. Żuchowski, *Phys. Rev. A* **92**, 022708 (2015).
- [17] H. Hara, Y. Takasu, Y. Yamaoka, J. M. Doyle, and Y. Takahashi, *Phys. Rev. Lett.* **106**, 205304 (2011).
- [18] F. Schäfer, H. Konishi, A. Bouscal, T. Yagami, and Y. Takahashi, *New J. Phys.* **19**, 103039 (2017).
- [19] F. Leroux, K. Pandey, R. Rehbi, F. Chevy, C. Miniatura, B. Grémaud, and D. Wilkowski, *Nat. Commun.* **9**, 3580 (2018).
- [20] F. Schäfer, N. Mizukami, P. Yu, S. Koibuchi, A. Bouscal, and Y. Takahashi, *Phys. Rev. A* **98**, 051602(R) (2018).
- [21] A. H. Hansen, A. Khramov, W. H. Dowd, A. O. Jamison, V. V. Ivanov, and S. Gupta, *Phys. Rev. A* **84**, 011606(R) (2011).
- [22] C. H. Schunck, M. W. Zwierlein, C. A. Stan, S. M. F. Raupach, W. Ketterle, A. Simoni, E. Tiesinga, C. J. Williams, and P. S. Julienne, *Phys. Rev. A* **71**, 045601 (2005).
- [23] S. Kotochigova, *Rep. Prog. Phys.* **77**, 093901 (2014).
- [24] M. B. Kosicki, M. Borkowski, and P. S. Żuchowski, *New J. Phys.* **22**, 023024 (2020).